An Optimal Information Method for Mobile Manipulator Dynamic Parameter Identification

Vivek A. Sujan and Steven Dubowsky, *Fellow, IEEE*

***Abstract*—High-performance robot-control algorithms often rely on system-dynamic models. For field robots, the dynamic parameters of these models may not be well known. This paper presents a mutual-information-based observability metric for the online dynamic parameter identification of a multibody system. The metric is used in an algorithm to optimally select the external excitation required by the dynamic system parameter identification process. The excitation is controlled so that the identification favors parameters that have the greatest uncertainty at any given time. This algorithm is applied to identify the vehicle and suspension parameters of a mobile-field manipulator, and is found to be computationally more efficient and robust to noise than conventional methods. Issues addressed include the development of appropriate vehicle models, compatible with the onboard sensors. Simulations and experimental results show the effectiveness of this algorithm.**

***Index Terms*—Dynamic parameter identification, field robots, information theory.**

I. Introduction

FUTURE mobile-field robotic systems, such as for planetary and terrestrial missions, will be required to perform complex tasks [12], [22]. Planetary robots will be used to collect rock samples, to build infrastructures, and explore complex terrains. Tasks for terrestrial field robots may include explosive ordinance removal, de-mining and handling hazardous waste, environment restoration [5], [12], [19], [22]. A field robot might be equipped with a manipulator arm and sensors such as inclinometers, accelerometers, vision systems, and force/torque sensors (see Fig. 1). Control algorithms for such systems have been proposed that rely on accurate physical models of the system and its tasks [11]. To successfully apply such algorithms, accurate estimates of the dynamic parameters of the system are required. These parameters may be often calculated from design data or found from laboratory tests. However, for field systems in hostile environments, handling unknown payloads, these estimates may not be accurate. For example, temperature fluctuations result in substantial changes in vehicle suspension stiffness and damping. Vehicle fuel consumption, the mass of rock samples collected, etc. can cause changes in the location of the center of gravity, the mass and the inertia of the system. Hence, online identification of these parameters can be critical for the system performance. This

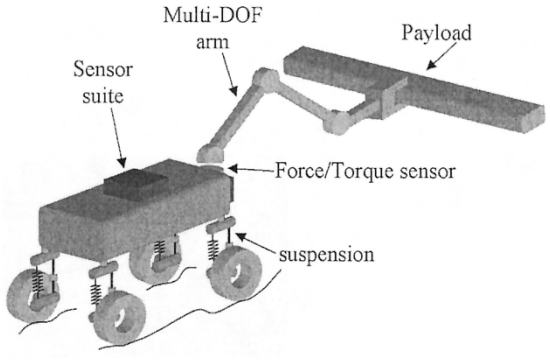

Fig. 1. Representation of a general mobile-field robot.

is a classical and well studied online identification problem: finding values of the parameters in the mathematical model of a system from online measured data such that the predicted dynamic response coincides with that of the real system [1], [3], [4], [13], [17], [18], [21], [20], [24].

Various effective algebraic and numerical solution techniques have been developed to solve for unknown parameters using dynamic system models [4], [7], [8], [17], [21]. These include techniques based on pseudo-inverses, Kalman observers, Levenberg–Marquardt methods, and others. The accuracy/quality of the identified system parameters is a function of both the excitation imposed on the system as well as the measurement noise (sensor noise). A number of researchers have developed metrics to evaluate the quality of the identified system parameters [2], [6], [20], [21], [24]. Such metrics determine if a given set of parameters is identifiable, which is known as the "identifiability/observability" problem [21]. These include tests based on differential algebra, where a set of differential polynomials describes the model under consideration [4], [13]. Other metrics monitor the condition number of an excitation matrix computed from the dynamic model. Examples of such excitation matrices include the Hessian of the model residual vector, the derivative of the system Hamiltonian, and the input correlation matrix [2], [6], [7], [21]. The metrics of parameter quality can be used to select the excitation imposed on the physical system and have been applied with limited success to industrial robotic systems [2], [3], [6], [7], [15].

However, such approaches can be computationally complex, an important issue for space robots where computational power is very limited. For example, defining excitation trajectories for the identification of an industrial 3-DOF manipulator using an input correlation matrix requires 40 h of VAX time [2], [6]. Additionally, these methods are unable to indicate which

Manuscript received August 1, 2002; revised January 20, 2003. Recommended by Guest Editors C. Mavroidis, E. Papadopoulos, and N. Sarkar.

The authors are with the Department of Mechanical Engineering, Massachusetts Institute of Technology, Cambridge, MA 02139 (e-mail: vasujan@mit.edu; dubowsky@mit.edu).

Digital Object Identifier 10.1109/TMECH.2003.812830

parameter estimates have low confidence values (low quality), since the quality metrics combines the performance into a single parameter. Thus, it is not possible to assign higher weight to parameters of greater dynamic significance to system response.

In this paper, a new mutual-information-based performance metric is presented for the online dynamic parameter identification of a multibody system. This metric measures the uncertainty of each parameter's estimate. This measure is termed here the "parameter observability." The metric is used to formulate a cost function that optimally controls the external excitation to effectively identify the system dynamic parameters. The cost function weighs each parameter estimate according to its uncertainty. Hence, the excitation is controlled so that the identification favors parameters that have the greatest uncertainty at any given time. This method is computationally more efficient and yields faster convergence than single parameter methods. Also, parameters may be given greater importance in the cost function based on its significance to the system's dynamic response.

Here, the algorithm is applied to the online parameter identification of a mobile-field robot system (such as one used for planetary exploration) and is shown to be computationally efficient. An onboard manipulator arm (with bandwidth constraints) is moved to generate reaction forces, which excite vehicle base motions. The dynamic parameters include the mass, location of center of gravity, the inertia, suspension/wheel compliance and damping. The method assumes that the robotic system itself is composed of rigid elements, and the vehicle wheels do not move (roll/slip) during the identification process. The algorithm also assumes that the robot is equipped with an inclinometer, an accelerometer and an arm base force/torque sensor. It is assumed that the onboard manipulator dynamic parameters are known and the bandwidth of the arm actuators is sufficiently high, to excite the vehicle dynamics. Finally, small motions of base compliance are assumed to occur. The system is modeled using a Newton–Euler formulation. A Kalman filter is used to solve the dynamic parameters based on the physical model. The mutual-information-based observability metric is used to determine the arm excitation trajectory. Simulation and experimental results show the effectiveness of this algorithm to identifying the system dynamic parameters [25].

II. Approach

As described above, the dynamic parameter identification algorithm consists of four parts. First, a vehicle spatial dynamic model is developed. This model is compatible with the onboard sensors in that the system state vector may be directly measured at any time. Secondly, the unknown dynamic parameters of this model are estimated using a Kalman filter, the dynamic model and a series of system–state vector measurements in response to a known external disturbance. Thirdly, the measurement uncertainty of a parameter at any given time (obtained from the Kalman filter) is used to formulate an observability measure of that parameter using a mutual-information-based metric. Finally, the current observability measures of each parameter are then combined to give a total observability cost function for the system. This cost function is optimally reduced by appropriately selecting the external disturbance. The current measures of the unknown parameters, the dynamic model and the Kalman filter are used to determine the direction of steepest descent for the cost function. This updated external disturbance is then applied to the system and the process is repeated until parameter estimate convergence is achieved. These four parts are now described in greater detail.

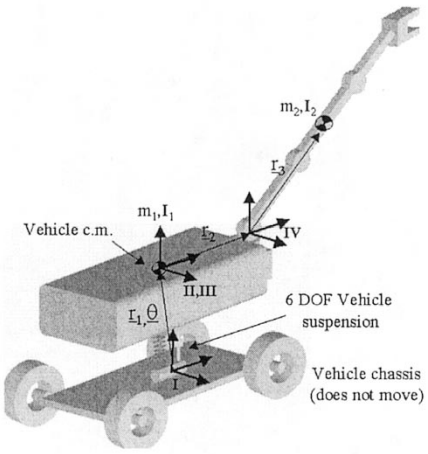

Fig. 2. Representation of the simplified mobile robot.

III. System-Dynamic Model

A number of models of vehicle-suspension systems have been proposed [1], [9], [10], [14], [16]. Many of these are quarter- or half-vehicle models that consider stiffness and damping coefficients, but neglect vehicle mass and inertial properties. Here, a Newton–Euler formulation is used to write the full spatial dynamics of the system. The system represented in Fig. 1, is reduced to three components: a rigid arm, a rigid vehicle body, and a suspension/wheel compliance module (see Fig. 2). Rotational motions of the rigid arm about an axis in frame IV [Fig. 3(a)] result in reaction forces/moments felt by the vehicle base [Fig. 3(b)] and in the suspension module (Fig. 4). Motions of the base are measured through the onboard inclinometer and accelerometer. Interaction forces/torques between the arm and the vehicle base are measured by a force/torque sensor (origin coincides with frame VI—Fig. 2).

The vehicle multi-element suspension system is represented by a 6-DOF linear stiffness and damping system, located at the vehicle base center-of-gravity. For small base motions, this model of suspension is sufficient to model the vehicle dynamics accurately. All coefficients of this model can be identified by only observing the vehicle base motions, thus eliminating the need for the placement of more exotic sensors at each individual suspension.

The spatial interaction forces/moments of the rigid arm are

$$\begin{aligned}(\mathbf{F}_{\mathbf{1,2}})_{IV}+(m_2\mathbf{g})_{IV}&=(m_2\mathbf{a}_{cm_2})_{IV}(\mathbf{N}_{1,2})_{IV}\\&\quad-(\mathbf{r}_3\times\mathbf{F}_{1,2})_{IV}\\&=\left(\frac{\partial(\mathbf{I}_2^{cm}\varpi_2^{cm})}{\partial t}+\varpi_2^{cm}\times(\mathbf{I}_2^{cm}\varpi_2^{cm})\right)_{IV}\end{aligned}$$

$$(\mathbf{F}_{1,2})_{IV}\text{and}\ (\mathbf{N}_{1,2})_{IV}\Rightarrow\text{from arm base } F/T \text{ sensor} \tag{1}$$

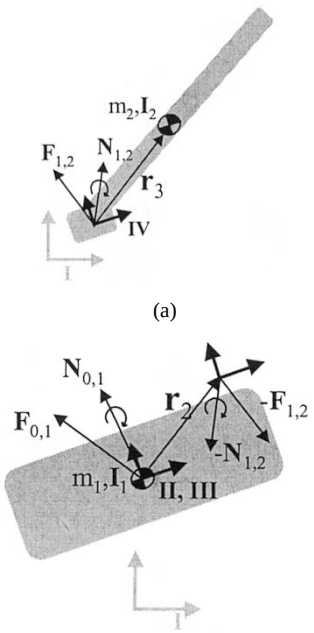

Fig. 3. Force/moment balance. (a) Rigid arm. (b) Vehicle base.

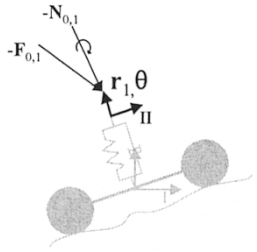

Fig. 4. Force/moment balance of compliance module.

where $\mathbf{F}_{12}$ and $\mathbf{N}_{12}$ are the reaction forces and moments, m_2 and $\mathbf{I}_2$ are the arm mass and inertia tensors, $\mathbf{a}_2$ and ω_2 are the arm linear acceleration and angular velocity vectors. The spatial interaction forces/moments of the rigid base are

$$(\mathbf{F}_{0,1})_{II} = (m_1\mathbf{a}_{cm_1})_{II} - (-\mathbf{F}_{1,2})_{II} - (m_1\mathbf{g})_{II}$$
$$(\mathbf{N}_{0,1})_{II} = \left(\frac{\partial(\mathbf{I}_1^{cm}\varpi_1^{cm})}{\partial t} + \varpi_1^{cm} \times (\mathbf{I}_1^{cm}\varpi_1^{cm})\right)_{II} - (-\mathbf{N}_{1,2})_{II} + (\mathbf{r}_2 \times \mathbf{F}_{1,2})_{II} \quad (2)$$

where $\mathbf{F}_{01}$ and $\mathbf{N}_{01}$ are the reaction forces and moments, m_1 and $\mathbf{I}_1$ are the base mass and inertia tensors, $\mathbf{a}_1$ and ω_1 are the base linear acceleration and angular velocity vectors.

Finally, the spatial interaction forces/moments of the suspension/wheel compliance module are given by

$$d(-\mathbf{F}_{0,1})_{II} = \mathbf{b}_{\overline{r}_1}^T \cdot d\dot{\mathbf{r}}_1 + \mathbf{k}_{\overline{r}_1}^T \cdot d(\mathbf{r}_1 - \mathbf{r}_1^0)$$
$$d(-\mathbf{N}_{0,1})_{II} = \mathbf{b}_{\overline{\theta}}^T \cdot d\dot{\boldsymbol{\theta}} + \mathbf{k}_{\overline{\theta}}^T \cdot d(\boldsymbol{\theta} - \boldsymbol{\theta}_0) \quad (3)$$

where $\mathbf{k}_r$ and $\mathbf{k}_\theta$ are the translational and rotational stiffness coefficients, and $\mathbf{b}_r$ and $\mathbf{b}_\theta$ are the translational and rotational damping coefficients. Using (1)–(3), a set of six dynamic equations is obtained (forces and moments in three dimensions)

$$m_1\left(d(\mathbf{R}_0^{-1}\mathbf{g}) - d(\ddot{\mathbf{r}}_1)_{II}\right) - \mathbf{b}_{\overline{r}_1}^T \cdot d\dot{\mathbf{r}}_1 - \mathbf{k}_{\overline{r}_1}^T \cdot d\mathbf{r}_1 = d(\mathbf{F}_{1,2})_{II} - \mathbf{I}_1 d(\ddot{\boldsymbol{\theta}})_{II} - d\left(\dot{\boldsymbol{\theta}} \times (\mathbf{I}_1\dot{\boldsymbol{\theta}})\right)_{II} - d(\mathbf{r}_2 \times \mathbf{F}_{1,2})_{II} - \mathbf{b}_{\overline{\theta}}^T \cdot d\dot{\boldsymbol{\theta}} - \mathbf{k}_{\overline{\theta}}^T \cdot d\boldsymbol{\theta} = d(\mathbf{N}_{1,2})_{II}. \quad (4)$$

Using the onboard sensors described above, this set of equations present the following unknowns, knowns, and measurable quantities:

unknowns: m_1, $\mathbf{I}_1$, $\mathbf{r}_2$, $\mathbf{k}_{\overline{r}_1}$, $\mathbf{b}_{\overline{r}_1}$, $\mathbf{k}_{\overline{\theta}}$, $\mathbf{b}_{\overline{\theta}}$

knowns: m_2, $\mathbf{I}_2$

measured: $d\mathbf{r}_1$, $d\dot{\mathbf{r}}_1$, $d\ddot{\mathbf{r}}_1(III$ w.r.t. $II)$, $d\boldsymbol{\theta}$, $d\dot{\boldsymbol{\theta}}$, $d\ddot{\boldsymbol{\theta}}$ $\cdot\,(II$ w.r.t. $I)$.

Note that only the linear velocities and its higher derivatives of the base can be computed from accelerometers and inclinometers. This dynamic model is compatible with this requirement. The sixdynamic equations of motion are evaluated for three rotation modes or the arm (rotation about the x, y and z axes) giving a total of 18 independent equations. Note that the arm rotation occurs only about the base joints. The remaining joints are held fixed. This configuration is sufficient to produce the dynamic forces required to generate the needed vehicle excitations for identification. This helps maintain the generality of the algorithm developed in this paper, as no specific manipulator kinematics are required other than two base rotational joints. Finally, note that the model assumes no relative motion between the wheel and soil. This constraint may be relaxed if additional sensors are added to measure vehicle motion due to soil slip or soil deformation. However, even for soft soil, soil stiffness is about three orders of magnitude higher than wheel tires (at 20-psi relative pressure). Further, on relatively flat surfaces, the vehicle slip is much smaller than motion due to suspension compliance. Thus, for vehicle parameter identification, the assumption that vehicle motions are dominated by suspension compliance is acceptable.

IV. Estimating Dynamic Parameters

Equation (4) can be cast into the form $\mathbf{A}\mathbf{x} = \mathbf{F}$ (where $\mathbf{A}$ is a known matrix, $\mathbf{x}$ is a vector of unknowns, and $\mathbf{F}$ is a known vector). Two common methods to solve such an equation are pseudo-inverses and Kalman filters. Both result in a least-squares solution.

In a pseudo-inverse solution process, a discrete set of measurements combined with the 18 equations is used to formulate the matrix $\mathbf{A}$ and the vector $\mathbf{F}$. A solution to $\mathbf{A}\mathbf{x} = \mathbf{F}$ is simply given by

$$\mathbf{x} = (\mathbf{A}^T\mathbf{A})^{-1}\mathbf{A}^T.\mathbf{F}.$$

A more efficient solution is to use a Kalman filter [8]. A Kalman filter is a multiple-input, multiple-output digital filter that can optimally estimate, in real time, the states of a system

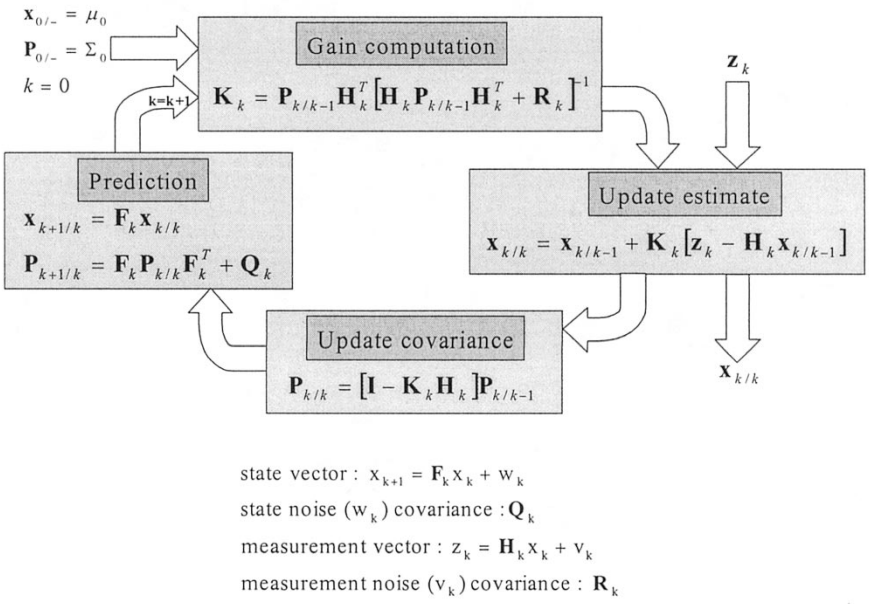

Fig. 5. Flow diagram of a Kalman filter.

based on its noisy outputs. These states are all the variables needed to completely describe the system behavior as a function of time. The measurements are statistically optimum in the sense that they minimize the mean-square estimation error. Here, rather than estimating $\mathbf{x}$ based on one large matrix $\mathbf{A}$ (containing all the measurements), $\mathbf{x}$ is estimated based on a single set of measurements and an associated covariance matrix is developed. With each new measurement set, the estimate is improved and the covariance updated (see Fig. 5).

There are numerous articles describing Kalman filters [4], [7], [8], [17]. In Fig. 5, Q_k models the uncertainty which corrupts the system model, R_k models the uncertainty associated with the measurement, and P_k gives total uncertainty of the state estimate. Initial conditions for the estimated parameters are set to initial design values (if known) or zero (if initial values are not known). The initial choice of the associated covariance matrix is set to the range of the sensors i.e., uncertainty is as large as the range of sensing.

V. Metric for Observability

While pseudo-inverse and Kalman filter methods produce estimates for the unknown dynamic parameters, finding a fundamental measure of accuracy of the current estimate for a given dynamic parameter is a difficult problem. To date, *a priori* tests to provide such a metric (called here the observability metric—which will be used by the identification algorithm) are not available. Although, classical definitions for parameter observability do exist, these do not account for measurement noise and are unable to determine the accuracy to which the parameter is known (Section V-I). To overcome these limitations, a new observability metric is developed (Section V-B). This metric is based on the average mutual information contained in the current estimate of a given parameter. This metric reflects how well any particular parameter is known.

A. Classical Observability Metric

The concept of observability in classical control is used to determine if there are a sufficient number of independent equations that relate the system states, and from which these states may be inferred. Formally, a system is observable if its initial state can be determined by observing its output for some finite period of time [4], [17]. This is briefly outlined below.

Given a linear system, a model (in the absence of a forcing function) can be written as

$$\begin{aligned} \dot{\overline{x}} &= \mathbf{F}\overline{x} + \mathbf{G}\overline{w} \quad \text{state model} \\ \overline{z} &= \mathbf{H}\overline{x} + \overline{v} \quad \text{observation model.} \end{aligned} \tag{5}$$

This continuous-time model can be transformed to the discrete model

$$\begin{aligned} \overline{x}_{k+1} &= \mathbf{\Phi}_k\overline{x}_k + \mathbf{\Gamma}_k\overline{w}_k \quad \text{state model} \\ \overline{z}_k &= \mathbf{H}_k\overline{x}_k + \overline{v}_k \quad \text{observation model} \end{aligned} \tag{6}$$

where

- $\overline{x}_k$ $(n \times 1)$ system state vector at time t_k;
- $\mathbf{\Phi}_k$ $(n \times n)$ transition matrix which relates $\overline{x}_k$ to $\overline{x}_{k+1}$;
- $\mathbf{\Gamma}_k$ $(n \times n)$ process noise distribution matrix;
- $\overline{w}_k$ $(n \times 1)$ white disturbance sequence with known covariance structure;
- $\overline{z}_k$ $(m \times 1)$ measurement at time t_k;
- $\mathbf{H}_k$ $(m \times n)$ measurement matrix or observation matrix;
- $\overline{v}_k$ $(m \times 1)$ white measurement noise sequence with known covariance.

If (5) is linear and $\mathbf{F}$ is constant in time, then the transition matrix is a function only of the time step dt, and is given by the matrix exponential

$$\mathbf{\Phi}_k = e^{\mathbf{F}\,\Delta t} = \mathbf{I} + \mathbf{F}\,\Delta t + \frac{(\mathbf{F}\,\Delta t)^2}{2!} + \cdots \tag{7}$$

It is assumed that process and measurement noise are uncorrelated in time (white) and with respect to each other. When dt is much smaller than the dominant time constants in the system, a two-term approximation of (7) is sufficient. In practice, the transition matrix can often be written by inspection.

Consider the discrete nth-order constant coefficient linear system, $\overline{x}_{k+1} = \mathbf{\Phi}_k \overline{x}_k$, for which there are m noise-free measurements, $z_k = \mathbf{H}x_k$ (where $k = 0 \cdots m-1$), where $\mathbf{H}$ is an $(m \times n)$ matrix [see (6)]. The sequence of the first i measurements can be written as

$$\begin{aligned} z_0 &= Hx_0 \\ z_1 &= Hx_1 = H\Phi x_0 \\ z_2 &= Hx_2 = H\Phi^2 x_0 \\ &\vdots \\ z_{i-1} &= Hx_{i-1} H\Phi^{i-1} x_0. \end{aligned} \tag{8}$$

This can be written as the augmented set of equations, $Z = \Xi^T x_0$ where $\Xi = [H^T | \Phi^T H^T | \cdots | (\Phi^T)^{n-1} H^T]$. If the initial state is to be determined from this sequence of measurements then Ξ must have rank n. This definition of observability is limited in that it does not account for the effects of corrupted (noise) data. Additionally, the unobservable state cannot be determined. To address both problems, a new observability metric is proposed below.

B. Mutual-Information-Based Observability Metric

For a given sensor (channel) transmitting a signal (measurement) y of a parameter x, the mutual information of x given y, reflects the information content (or certainty) of the current measurement with respect to the true parameter value. Here, the sensor may be *physical* (such as an inclinometer), or *conceptual* (measurement is derived from physical sensors and constitutive relationships—such as the output of a Kalman filter). The signal being read by the sensor (x) is the true value of the unknown dynamic parameter to be identified. The signal being transmitted by the sensor (y) is the value of the unknown parameter provided to a computer corrupted by noise. Essentially, the amount of information about an unknown parameter x being transmitted by a channel gives the measure of observability of that parameter. This metric reflects how well any particular parameter is known. This derivation is briefly outlined below.

For a discrete (digital) channel there exists a finite set of possible output states determined by the sensor resolution. Assume that this set of possible output states have known probabilities of occurrence $(p_1, p_2, \ldots, p_n)$ independent of the input. If there is a measure of the amount of uncertainty (or lack of information) in predicting the output of a sample from the channel given these probabilities $H(p_1, p_2, \ldots, p_n)$, it is reasonable to require of it the following properties [23].

1) Continuity—H should be continuous in p_i.
2) Maximal—If all the p_i are equal, $p_i = 1/n$, then H should be a monotonic increasing function of n.
3) Additive—If a choice be broken down into two successive choices, the original H should be the weighted sum of the individual values of H.

It has been shown that the only H satisfying the three assumptions is of the form (where K is a positive constant) [23]

$$H = -K \sum_{i=1}^{n} p_i \log p_i. \tag{9}$$

More generally, for a finite number of input and output states, a set of probabilities is assumed: $p_\alpha(\beta)$. This is the probability of a transmitted state α being received as state β [23]. A number of important uncertainty measures can be calculated: the uncertainty of the input of the channel, $H(x)$; the uncertainty of the output of the channel, $H(y)$; the joint uncertainty of input and output of the channel, $H(x, y)$; the conditional uncertainty of the output when the input is known and conversely, $H(y|x)$ and $H(x|y)$. In the noiseless case $H(y) = H(x)$. Now, consider the case where the signal is perturbed by noise during transmission i.e., the received signal is not necessarily the same as that sent out by the transmitter—or the true value of an unknown parameter is not the same as its estimate. In this case the received signal, y, is a function of the transmitted signal, x, and a second variable, the noise n: $y = f(x, n)$. The noise is represented by a suitable stochastic process, $p(x_i, y_j)\ 1 \le i \le N, 1 \le j \le M$ (where N, M is the number if discrete sensor input and output states). Thus, if a noisy channel is fed by a source there are two statistical processes at work: the source and the noise. Thus, the conditional entropy of x given y is defined as [23]

$$H(\mathbf{x}|\mathbf{y}) = -\sum_{i=1}^{N} \sum_{j=1}^{M} p(x_i, y_j) \log_2 p(x_i|y_j). \tag{10}$$

Some important properties of the conditional entropy can be derived [23] as follows.

i) $H(x|y) \le H(x)$ with equality if and only if x and y are independent.
ii) $H(x, y) = H(y) + H(x|y) = H(x) + H(y|x)$.

All these can be calculated on a per-second basis. These uncertainties are used to get an estimate on the amount of information being transmitted by such a sensor i.e., the measure for observability. Recall that the input signal is the true value of the unknown parameter being identified. The signal transmitted is the value that the sensor provides as an estimate of the unknown parameter corrupted by noise. For the random variables x and y with joint probability distribution $p(x_i, y_j)$ for a single channel, the average amount of information (or certainty) about x contained in y is defined in terms of the reduction in the uncertainty of x by measuring y. Denoting this information by $In(x, y)$, define

$$In(x, y) = H(x) - H(x|y). \tag{11}$$

With property ii), it is easy to show that

$$In(y, x) = H(y) - H(y|x) = In(x, y). \tag{12}$$

Thus, the information about x contained in y is equal to the information about y contained in x. For this reason, $In(x, y)$ is called the average mutual information between x and y. From property i), $In(x, y) \ge 0$ with equality if and only if x and y

are independent. As a direct consequence of the definition of $In(x, y)$

$$In(x, y) = \sum_{i=1}^{N} \sum_{j=1}^{M} p(x_i, y_j) \log_2 \frac{p(x_i, y_j)}{p(x_i)p(y_j)}. \tag{13}$$

To develop the relationship $p(x_i, y_j)$, sensor noise is now modeled. A single observation of x is modeled as a Gaussian probability distribution centered at y. A Gaussian-to-model uncertainty in sensor output is based on two important observations. The use of the mean and the covariance of a probability distribution function is a reasonable form to model sensor output and is a second-order linear approximation. This linear approximation corresponds to the use of a Gaussian function with all higher moments equal to zero. Additionally, based on the central limit theorem, the sum of a large number of independent variables has a Gaussian distribution regardless of their individual distributions [26]. For example, the canonical form of the Gaussian distribution for three spatial dimensions (x, y, z) depends on the standard deviations of the measurement, $\sigma_{x,y,z}$, a covariance matrix (C) and the mean measurement ($\overline{y}$) [13], [17], [27]

$$p(\overline{x}'|\overline{y}) = \frac{1}{(2\pi)^{n/2}\sqrt{|C|}} \exp\left(-\frac{1}{2}(\overline{y} - \overline{x}')^T C^{-1}(\overline{y} - \overline{x}')\right)$$

where

$$C = \begin{bmatrix} \sigma_x^2 & \rho_{xy}\sigma_{xy}\sigma_{xy} & \rho_{zx}\sigma_{zx}\sigma_{zx} \\ \rho_{xy}\sigma_{xy}\sigma_{xy} & \sigma_y^2 & \rho_{yz}\sigma_{yz}\sigma_{yz} \\ \rho_{zx}\sigma_{zx}\sigma_{zx} & \rho_{yz}\sigma_{yz}\sigma_{yz} & \sigma_z^2 \end{bmatrix} \tag{14}$$

where the exponent is called the Mahalanobis distance. For uncorrelated measured data $\rho = 0$. This can be generalized for any dimensional sensor. $H(x)$ and $H(x|y)$ can be explicitly defined in terms of a given sensor

$$H(x) = \sum_{i=1}^{n} p_i \log p_i \tag{15a}$$

where, for example in a special case of a discrete sensor $p_i = 1/n$ and $n =$ number of sensor discrete states

$$H(x|y) = \sum_{i=0}^{n-1} q_i \log q_i \quad \text{where} \quad q_i = \frac{\int_a^b p(\overline{x}'|\overline{y})\, d\overline{x}'}{\max \int_{\min} p(\overline{x}'|\overline{y})\, d\overline{x}'}$$

and

$$\begin{cases} a = \min + i\left(\dfrac{\max - \min}{n}\right) \\ b = \min + (i+1)\left(\dfrac{\max - \min}{n}\right) \\ \max = \text{ maximum sensor reading} \\ \min = \text{ minimum sensor reading} \\ p(\overline{x}'|\overline{y}) \text{ is obtained from (2)–(11).} \end{cases} \tag{15b}$$

Thus, $In(y, x)$ in(13) reflects the information content of the current estimate of the dynamic parameter being estimated. In other words, increasing certainty of a parameter estimate is reflected in the increasing value of $In(y, x)$ associated with that parameter (known as In_{x_i} for the x_i parameter). This metric makes no assumption on the noise statistics (Gaussian, etc.). It is convenient to establish the details using Gaussian noise.

VI. Formulation of Exciting Trajectories

Formulating an appropriate arm-exciting trajectory is based on using the estimate of the dynamic parameters combined with the observability metric (from Section V). The observability metrics for each of the unknown parameters is combined into a total observability cost function for the system. This cost function is optimally reduced by appropriately selecting the external disturbance—arm motion. This is achieved by determining the expected observability metrics associated with each of the unknown parameters using the current measures of the unknown parameters, the system dynamic model, the Kalman filter and the external excitation. These expected metric values are used to optimally reduce the observability cost function in the direction of steepest descent. This results in an updated external disturbance that is then applied to the system and the process is repeated until parameter estimate convergence is achieved. The following describes this process in detail.

From Section III a set of differential algebraic equations of motion of the form: $\mathbf{Ax} = \mathbf{F}$ is obtained. For the robot system the arm excitation is sinusoidal, namely $f(t) = a_0 + a.\sin(\omega t)$ [(1)]. The control parameters vector $\mathbf{d} \in R^3$ consists of the amplitude (a), frequency (ω) and offset (a_0) of motion of the robotic arm.

Based on the associated observability metric (Section V) for each of the dynamic parameter estimates, $\tilde{x}_k$, an observability cost function $V(\mathbf{d})$ is defined as follows:

$$\begin{aligned} V(\mathbf{d}) &= \frac{1}{2}\sum_i \left(1 - \left(1 - \frac{In_{x_i}}{In_{x_i}^{\max}}\right)\frac{In_{x_i}}{In_{x_i}^{\max}}\right) \\ &= \frac{1}{2}\sum_i 1 - \frac{In_{x_i}}{In_{x_i}^{\max}} + \left(\frac{In_{x_i}}{In_{x_i}^{\max}}\right)^2 \\ &\equiv \tfrac{1}{2}\sum_i r_i^2(\mathbf{d}) \end{aligned} \tag{16}$$

where i is summed over the number of dynamic parameters to be identified. In_{x_i} is the current information associated with parameter estimate x_i. $In_{x_i}^{\max}$ is the current maximum information (observability) associated with any of the parameter estimates. In this cost function the information associated with each parameter is weighted such that parameters with a higher uncertainty receive a higher weight. Although this particular choice of cost function biases the identification algorithm toward the more uncertain parameters, this may be easily amended to include weightings that reflect the relative importance of the individual dynamic parameters or other weightings that may be problem dependent.

A numerical minimization routine is applied to this observability cost function. By assembling the terms $r_i(\mathbf{d})$ [see (16)] into a vector $\mathbf{R}(\mathbf{d})$, given as

$$\mathbf{R}(\mathbf{d}) = \{r_1(\mathbf{d}), \ldots, r_n(\mathbf{d})\}^T \tag{17}$$

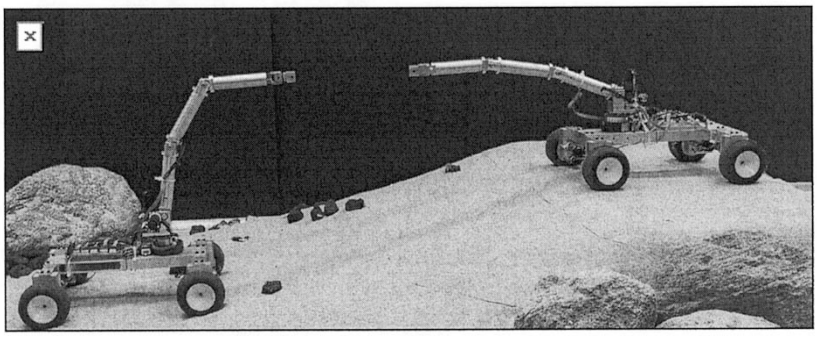

Fig. 6. Experimental mobile manipulator systems.

the control parameters $\mathbf{d}$ must be chosen so that the magnitude of $\mathbf{R}$ is minimized. The quadratic cost function $V(\mathbf{d})$ of (16) becomes

$$V(\mathbf{d}) = \tfrac{1}{2}\,\mathbf{R^T}(\mathbf{d})\mathbf{R}(\mathbf{d}). \tag{18}$$

The problem of finding $\mathbf{d}$ from $V(\mathbf{d})$ is a nonlinear least-squares problem [17]. If the vector $R(\mathbf{d})$, is continuous, and if both first and second-order derivatives are available, then the nonlinear least-squares problem can be solved by standard unconstrained optimization methods [21]. Otherwise, a method that requires only the first derivatives of $R(\mathbf{d})$ must be used. The first derivative of (18) with respect to the design parameters, $\mathbf{d}$, is defined as

$$G(\mathbf{d}) = \sum_{i=1}^{n_m} \nabla r_i(\mathbf{d}) r_i(\mathbf{d}) = \mathbf{J}^T(\mathbf{d})\mathbf{R}(\mathbf{d}) \tag{19}$$

where $\mathbf{J}(\mathbf{d}) \in R^{n_m \times 3}$ is the Jacobian matrix of $R(\mathbf{d})$ with respect to the control parameters. The second derivative of (18) with respect to the control parameters, $\mathbf{d}$, is defined as

$$\begin{aligned} H(\mathbf{d}) &= \sum_{i=1}^{n_m} \left[\nabla r_i(\mathbf{d}) r_i(\mathbf{d})^T + \nabla^2 r_i(\mathbf{d}) r_i(\mathbf{d})\right] \\ &= \mathbf{J}^T(\mathbf{d})\mathbf{J}(\mathbf{d}) + \mathbf{S}(\mathbf{d}) \end{aligned} \tag{20}$$

where $\mathbf{S}(\mathbf{d}) \in R^{3\times 3}$ is part of $H(\mathbf{d})$ that is a function of second derivatives of $R(\mathbf{d})$. Thus, the knowledge of $J(\mathbf{d})$ supplies $G(\mathbf{d})$ and the part of $H(\mathbf{d})$ dependent on first-order derivative information, but not on the second-order part $S(\mathbf{d})$. Levenberg–Marquardt methods, applied in this work, simply omit $S(\mathbf{d})$ and base the step selection $(\mathbf{d}')$ on the approximation given by [21]

$$V(\mathbf{d}+\mathbf{d}') = V(\mathbf{d}) + G^T(\mathbf{d})\mathbf{d}' + \tfrac{1}{2}\,\mathbf{d}'\mathbf{J^T}(\mathbf{d})\mathbf{J}(\mathbf{d})\mathbf{d}'. \tag{21}$$

Equation (21) leads to the following optimization procedure:

$$\mathbf{d}^{(k+1)} = \mathbf{d}^{(k)} + \alpha_k \mathbf{d}'^{(k)} \tag{22}$$

with

$$\begin{aligned} \mathbf{d}'^{(k)} &= \frac{-G\left(\mathbf{d}^{(k)}\right)}{\mathbf{J}^T\left(\mathbf{d}^{(k)}\right)\mathbf{J}\left(\mathbf{d}^{(k)}\right)} \\ \alpha_k &= \arg\min_{\alpha}\left[V(\mathbf{d}^{(k)} + \alpha \mathbf{d}'^{(k)}\right] \end{aligned} \tag{23}$$

$\mathbf{d}'^{(k)}$ given by (23) represents the steepest descent direction of $V(\mathbf{d})$. Thus, using (22) and (23), the control parameters of the robot arm is refined during the identification process, leading to an optimal excitation trajectory. During this optimization process, $V(\mathbf{d})$ and its derivatives are computed based on the applying the excitation control parameters, d, to the system model and computing the expected system response. These responses are then used to compute the observability metric associated with each of the unknown parameters. This results in an updated external disturbance that is applied to the system and the process described in Section II is repeated till parameter estimate convergence is achieved.

VII. Results

A. Simulation

The mobile robot used in the simulation studies are modeled after the experimental system (see Fig. 6). Here, the parameter identification results for two tests using a three-dimensional simulation of a mobile robot system with a manipulator and suspension compliance are presented. The first uses a constant-parameter arm motion and the second uses a variable-parameter excitation function for arm motion. For constant-parameter arm motion, the arm is constrained to move sinusoidally, with no changes in frequency, amplitude and motion offset. For variable-parameter arm motion, the arm motion changes based on the formulation in Section VI. Both methods use a Kalman filter to make estimates on the unknown parameters. The parameter identification results are compared. The system is simulated for 10 s. The manipulator arm mass is assumed to be 1 kg and inertia $I_x = 0.02$ kg·m^2, $I_y = 0.001$ kg·m^2, $I_z = 0.02$ kg·m^2, $I_{xz} = 0$ kg·m^2, $I_{yz} = 0$ kg·m^2, and $I_{xy} = 0$ kg·m^2. In the simulation, sensor data are corrupted by adding white noise of up to 10% of the maximum sensed value. The evaluation of the observability metric and adjustment of the arm motion occur every 0.4 s, with a sampling time of 0.005 s.

The constant parameter excitation function is given by

$$f(t) = a_0 + a.\sin(\omega t) = \pi/4 + 2\pi/9.\sin(\pi/2t). \tag{24}$$

The mean control parameter values from the variable parameter case were selected for the excitation function for the constant control parameter case. Figs. 7 and 8 show the arm excitation functions for the two test cases. For a sensor with n-bit precision (i.e., 2^n possible values), the maximum value of the

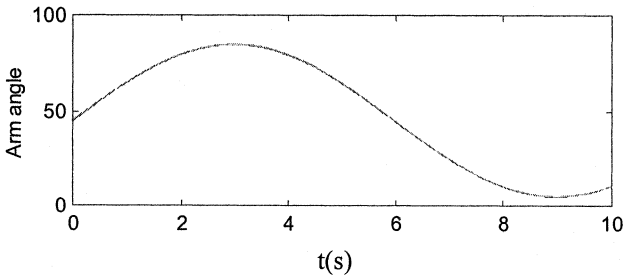

Fig. 7. Constant-parameter arm motion.

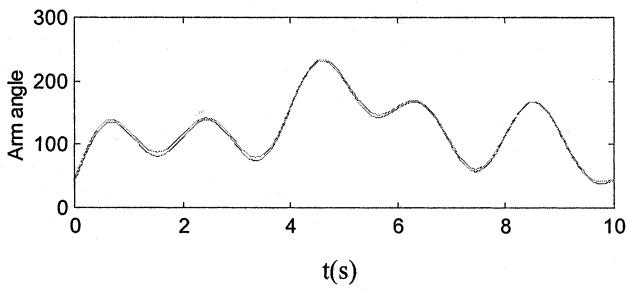

Fig. 8. Variable-parameter arm motion.

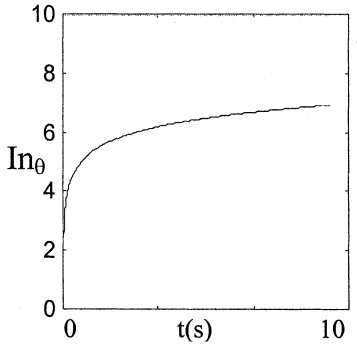

(a)

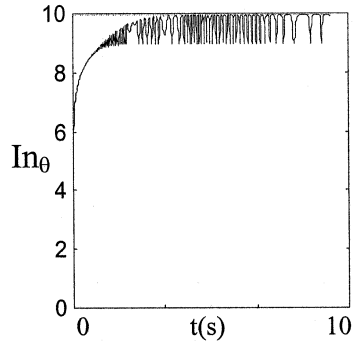

(b)

Fig. 9. Observability metric values for stiffness θ_p. (a) Constant-parameter excitation function. (b) Variable-parameter excitation function.

observability metric associated with the reading is n bits [i.e., no uncertainty, see (12)]. In both test cases, a 10-bit accuracy sensor is assumed i.e., 2^{10} possible values. Fig. 9 shows the value for the observability metric in identifying the stiffness in θ_p for the two test cases. It is seen that by using the variable-parameter excitation function (as opposed to constant-parameter excitation function), the amount of information associated with the unknown parameter In_θ, has low uncertainty (i.e., identified parameter value has high quality). Fig. 10 shows the convergence in identification of two parameters for the two test cases as a function of the number of sampling/evaluation steps. In general, using the variable-parameter excitation function results in faster and more accurate convergence of the estimates to the true values. Table I presents the identification results of the 22 unknowns (see Section III) using both arm excitation tests. The average percentage error shows an improvement of almost a factor of six for the variable parameter over the constant-parameter excitation function. The average computational time per evaluation step for 22 unknown parameters with $In_{x_i}^{\max} = 10$ bits on a PIII 750 MHz platform is 75 ms.

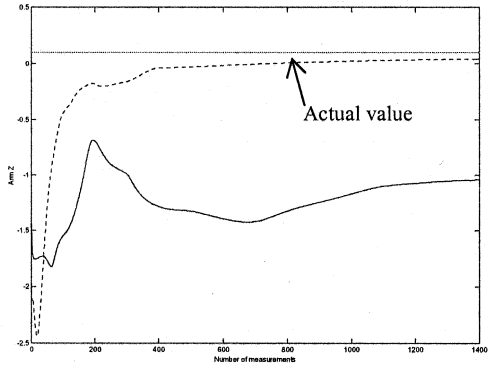

(a)

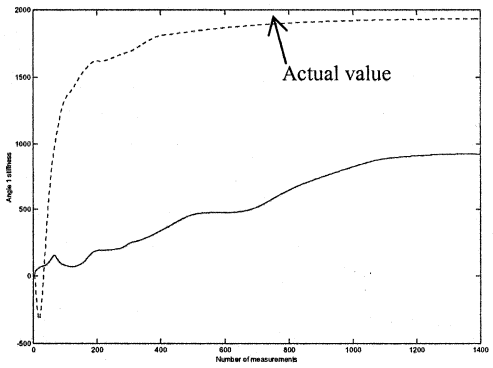

(b)

Fig. 10. Example of identification converge curves (– – – variable control parameters, — fixed control parameters). (a) c.g. Z. (b) Stiffness θ_p.

For comparison, the simulation is also run using a parameter quality metric based on the condition number of a matrix formed by the sensed values (matrix $\mathbf{A}$ in Section IV) [2]. The arm motion is refined to generate lower condition numbers (i.e., matrix $\mathbf{A}$ is better behaved). Although convergence results are similar for the unknown parameters, however, on average the parameter estimates converge an order of magnitude faster (in simulation time) using the information theory-based quality metric presented in this paper.

B. Experimental Studies

Experiments were performed on a laboratory four-wheeled robot with a four DOF manipulator arm mounted on a 6-axis

TABLE I
SIMULATION PARAMETER IDENTIFICATION

Parameter	True value	Constant parameter excitation function	Variable parameter excitation function
Mass (kg)	3.0	4.0	3.6
Inertia I_x (kg-m^2)	0.15	0.12	0.14
Inertia I_y (kg-m^2)	0.10	0.05	0.09
Inertia I_z (kg-m^2)	0.20	0.12	0.18
Inertia I_{xz} (kg-m^2)	0.0	0.05	0.01
Inertia I_{yz} (kg-m^2)	0.03	0.07	0.04
Inertia I_{xy} (kg-m^2)	0.0	0.04	0.01
c.g. x (m)	0.01	0.03	0.01
c.g. y (m)	0.3	0.5	0.3
c.g. z (m)	0.1	-1.1	0.1
Damping x (kg/s)	100	142	78
Damping y (kg/s)	100	140	76
Damping z (kg/s)	300	22	17
Damping θ_p (kg/s)	200	79	195
Damping θ_r (kg/s)	300	105	266
Damping θ_y (kg/s)	400	134	334
Stiffness x (kg/s^2)	1000	1103	979
Stiffness y (kg/s^2)	1000	1095	1244
Stiffness z (kg/s^2)	500	390	375
Stiffness θ_p (kg/s^2)	2000	945	1934
Stiffness θ_r (kg/s^2)	2500	1950	2394
Stiffness θ_y (kg/s^2)	3000	2403	2892
% Avg. Error		**108.8**	**18.9**

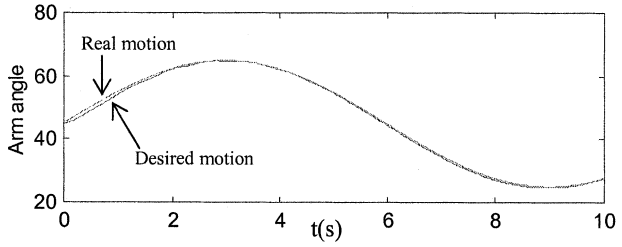

Fig. 11. Constant-parameter arm motion.

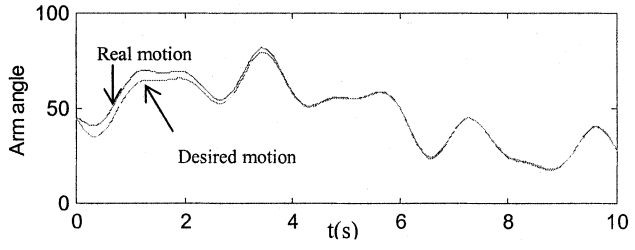

Fig. 12. Variable-parameter arm motion.

force/torque sensor (see Fig. 6). On-board sensors also include a two-axis inclinometer. A Pentium 166-MHz computer is used for real-time control, data acquisition, and data processing. All programs are written in C++ operating on Windows NT. The experimental system does not have an accelerometer, hence the identification process is limited to rotational dynamic components (inertia, stiffness, damping of roll/pitch axes and the location of the center of gravity).

The actual dynamic parameters were identified to serve as the basis for evaluating the method. The Mass was measured using a precision weighing scale. The location of the center of mass was found by titling the vehicle on one axis supported at two points, and measuring the reaction forces at the support points. Inertia was measured using pendulum oscillatory tests. Stiffness was measured by measuring deflection as a function of added load. Damping was measured by fitting the impulse response of the system to a second-order equation. Linear models were used for stiffness and damping tests. The force/torque sensor in the experimental system eliminates the need to measure the actual arm inertia tensor [see (4)].

Experimental results presented here are for the constant parameter and the variable-parameter arm excitation function. The experiments were run for approximately 10 seconds. Figs. 11 and 12 show the arm excitation functions for the two test cases.

Table II presents the identification results of the five unknowns using both arm excitation tests. The average percentage error shows an improvement of almost a factor of 8 for the variable parameter over the constant-parameter excitation function. Fig. 13 shows the convergence in identification of two parameters for the two test cases discussed here. In addition to the significant corruption of data due to sensor noise, inaccuracies in laboratory measurements of "true" vehicle dynamic parameters contribute to the errors seen.

VIII. CONCLUSION

This paper presents an algorithm based on a mutual information theoretic metric for the excitation of vehicle dynamics, to

TABLE II
EXPERIMENTAL PARAMETER IDENTIFICATION

Parameter	True value	Constant parameter excitation function	Variable parameter excitation function
Inertia x	0.072	0.04	0.04
c.g. y	0.054356	-0.07	0.07
c.g. z	0.036195	-0.09	0.05
Damping θ_p	1.5	7.5	1.5
Stiffness θ_p	317.0	355	327
% Avg. Error		**208.4**	**26.8**

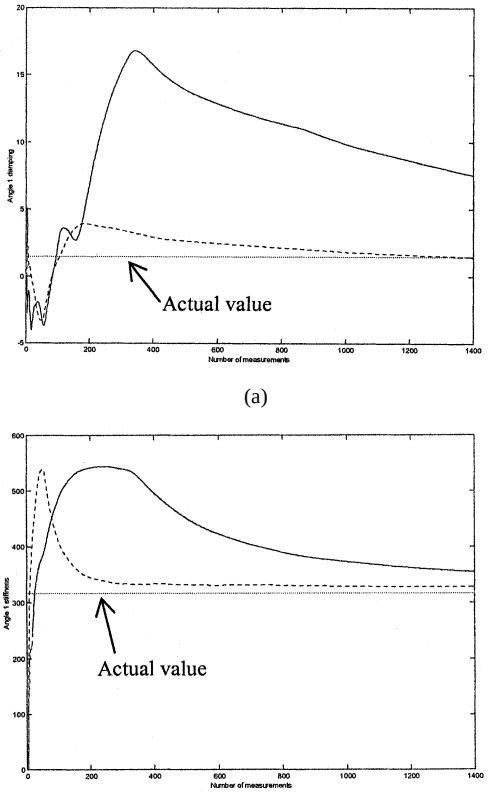

Fig. 13. Example of identification converge curves (– – – variable control parameters, — fixed control parameters). (a) Damping θ_p. (b) Stiffness θ_p.

efficiently estimate the dynamic parameters of mobile robots. In particular the vehicle inertial and compliance (suspension and tires) parameters are identified. The algorithm uses the onboard robotic arm to generate base motions, which are measured with simple onboard sensors, and fit to a physical model, thus obtaining estimates for the unknown parameters. The mutual-information-based metric measures the uncertainty of each parameter's estimate. This measure is termed here the "parameter observability." The metric is used to optimally select the external excitation required to excite the dynamic system effectively. The excitation is controlled so that the identification favors parameters that have the greatest uncertainty at any given time. The algorithm is applied to identify the vehicle and suspension parameters of a mobile-field manipulator, and is found to be computationally more efficient and robust to noise than conventional methods. Simulations and experimental results show the effectiveness of this algorithm.

ACKNOWLEDGMENT

The authors would like to acknowledge the support of the Jet Propulsion Laboratory, NASA in this work (in particular Dr. P. Schenker and Dr. T. Huntsberger). The authors also acknowledge the help of G. Kristofek, MIT, for the fabrication of the experimental system used in this work.

REFERENCES

[1] A. Alloum, A. Charara, and H. Machkour, "Parameters nonlinear identification for vehicle's model," in *Proc. IEEE Int. Conf. Control Applications*, vol. 2, Hartford, CT, Oct. 1997, pp. 1484–1489.
[2] B. Armstrong, "On finding exciting trajectories for identification experiments involving systems with nonlinear dynamics," *Int. J. Robot. Res.*, vol. 8, no. 6, pp. 28–48, 1989.
[3] C. G. Atkeson, C. H. An, and J. M. Hollerbach, "Estimation of inertial parameters of manipulator loads and links," *Int. J. Robot. Res.*, vol. 5, no. 3, pp. 101–119, 1986.
[4] Y. Bard, *Nonlinear Parameter Estimation*. London, U.K.: Academic Press, 1974.
[5] E. T. Baumgartner, P. S. Schenker, C. Leger, and T. L. Huntsberger, "Sensor-fused navigation and manipulation from a planetary rover," in *Proc. SPIE Symp. on Sensor Fusion and Decentralized Control in Robotic Sys.*, Boston, MA, Nov. 1998, pp. 2–15.
[6] M. Gautier and W. Khalil, "Exciting trajectories for the identification of base inertial parameters of robots," *Int. J. Robot. Res.*, vol. 2, no. 4, pp. 362–375, 1992.
[7] M. Gautier and Ph. Poignet, "Extended Kalman filtering and weighted least squares dynamic identification of robot," *Contr. Eng. Practice*, vol. 9, no. 12, pp. 1361–1372, 2001.
[8] A. Gelb, *Applied Optimal Estimation*. Cambridge, MA: MIT Press, 1974.
[9] C. Halfmann, O. Nelles, and H. Holzmann, "Modeling and identification of the vehicle suspension characteristics using local linear model trees," in *Proc. IEEE Int. Conf. on Control Applications*, vol. 2, Hawaii, HI, Aug. 1999, pp. 1484–1489.
[10] C. J. Harris, Z. Q. Wu, and Q. Gan, "Neurofuzzy state estimators and their applications," in *Proc. IEEE Colloq. Advances in Control Technology*, London, U.K., May 1999, pp. S1–S10.
[11] N. A. M. Hootsman, S. Dubowsky, and P. Z. Mo, "The experimental performance of a mobile manipulator control algorithm," in *Proc. IEEE Int. Conf. Robotics and Automation*, vol. 3, Nice, France, May 1992, pp. 1948–1954.
[12] T. L. Huntsberger, "Autonomous multi-rover system for complex planetary retrieval operations," in *Proc. SPIE Symp. Sensor Fusion and Decentralized Control in Autonomous Robotic Agents*, Pittsburgh, PA, Oct. 1997, pp. 220–229.
[13] L. Ljung and T. Glad, "Testing global identifiability for arbitrary model parameterizations," in *Identification and System Parameter Estimation*. New York: Pergamon, 1991, vol. 1/2, pp. 1077–1082.
[14] R. Majjad, "Estimation of suspension parameters," in *Proc. IEEE Int. Conf. Control Applications*, Hartford, CT, Oct. 1997, pp. 522–527.
[15] H. Mayeda, K. Yoshida, and K. Osuka, "Base parameters of manipulator dynamics," in *Proc. IEEE Int. Conf. Robotics and Automation*, vol. 3, Philadelphia, PA, Apr. 1988, pp. 1367–1372.
[16] O. Nelles and R. Isermann, "Basis function networks for interpolation of local linear models," in *Proc. IEEE Conf. Decision and Control*, vol. 1, Kobe, Japan, Dec. 1996, pp. 470–475.
[17] P. E. Nikravesh, *Computer-Aided Analysis of Mechanical Systems*. Englewood Cliffs, NJ: Prentice-Hall, 1988.

[18] H. B. Olsen and G. A. Beckey, "Identification of parameters in models of robots with rotary joints," in *Proc. IEEE Int. Conf. Robotics and Automation*, vol. 2, St. Louis, MI, Mar. 1985, pp. 1045–1049.
[19] J. F. Osborn, W.L Whittaker, K. Dowling, and S. Singh, "Robots for unstructured environments," *J. Unmanned Syst.*, vol. 8, no. 1, pp. 21–31, 1990.
[20] T. Schmidt and P. C. Muller, "A parameter estimation method for multibody systems with constraints," in *Advanced Multibody System Dynamics: Simulation and Software Tools*. Norwell, MA: Kluwer, 1993, pp. 427–432.
[21] R. Serban and J. S. Freeman, "Identification and identifiability of unknown parameters in multibody dynamic systems," *Multibody Syst. Dyn.*, vol. 5, no. 4, pp. 335–350, 2001.
[22] G. Shaffer and A. Stentz, "A robotic system for underground coal mining," in *Proc. IEEE Int. Conf. Robotics and Automation*, vol. 1, 1992, pp. 633–638.
[23] C. E. Shannon, "A mathematical theory of communication," *Bell Sys. Tech. J.*, vol. 27, pp. 379–423 and 623–656, 1948.
[24] T. Soderstorm and P. Stocia, *System Identification*. London, U.K.: Prentice-Hall International, 1989.
[25] V. A. Sujan, "Compensating for model uncertainty in the control of cooperative field robots," Ph.D. dissertation, Dept. of Mechanical Engineering, Massachusetts Institute of Technology, Cambridge, MA, June 2002.
[26] A. Kelly, *Introduction to Mobile Robotics*. Pittsburgh, PA: Carnegie-Mellon Univ., 1999.
[27] R. C. Smith and P. Cheeseman, "On the representation and estimation of spatial uncertainty," in *Int. J. Robot. Res.*, 1986, vol. 5, pp. 56–68.

Vivek Sujan received the B.S. degree in physics and mathematics *summa cum laude* from the Ohio Wesleyan University, Delaware, in 1996, the B.S. degree in mechanical engineering, with honors from the California Institute of Technology, Pasadena, in 1996, and the M.S. and Ph.D. degrees in mechanical engineering from the Massachusetts Institute of Technology (MIT), Cambridge, in 1998 and 2002, respectively.

He is currently a Post-Doctoral Associate in Mechanical Engineering at MIT. His research interests include the design, dynamics, and control of electromechanical systems; mobile robots and manipulator systems; optical systems and sensor fusion for robot control; and image analysis and processing.

Dr. Sujan is a member of Sigma Xi, Tau Beta Pi, Phi Beta Kappa, Sigma Pi Sigma, and Pi Mu Epsilon.

Steven Dubowsky (M'72–SM'99–F'01) received the Bachelor's degree from Rensselaer Polytechnic institute, Troy, NY in 1963, and the M.S. and Sc.D. degrees from Columbia University, New York, in 1964 and 1971, respectively.

He is currently a Professor of Mechanical Engineering at the Massachusetts Institute of Technology (MIT), Cambridge. He has been a Professor of Engineering and Applied Science at the University of California, Los Angeles, a Visiting Professor at Cambridge University, Cambridge, U.K., and Visiting Professor at the California Institute of Technology, Pasadena. Between 1963 and 1971, he worked with Perkin–Elmer Corporation, Wilton, CT, the General Dynamics Corporation, Falls Church, VA, and the American Electric Power Service Corporation, Roanoke, VA. His research has included the development of modeling techniques for manipulator flexibility, and the development of optimal and self-learning adaptive control procedures for rigid and flexible robotic manipulators. He has authored or coauthored nearly 200 papers in the areas of the dynamics, control and design of high performance mechanical and electromechanical systems.

Prof. Dubowsky is a Registered Professional Engineer in the State of California and has served as an Advisor to the National Science Foundation, and the National Academy of Science/Engineering, the Department of Energy, and the US Army. He is a Fellow of the ASME and a member of Sigma Xi and Tau Beta Pi.